MATERIALS CHEMISTRY
FRONTIERS

RESEARCH ARTICLE

View Article Online
View Journal | View Issue

Cite this: *Mater. Chem. Front.*, 2019, **3**, 1238

Light-triggered reversible disassembly of stimuli-responsive coordination metallosupramolecular Pd_2L_4 cages mediated by azobenzene-containing ligands†

Shuang Fu, Quan Luo, Mingsong Zang, Jun Tian, Zherui Zhang, Minghao Zeng, Yuancheng Ji, Jiayun Xu and Junqiu Liu *

Received 16th March 2019,
Accepted 17th April 2019

DOI: 10.1039/c9qm00160c

rsc.li/frontiers-materials

Herein, a new light stimuli-responsive supramolecular metal–organic coordination M_2L_4 azo-cage with lantern-shaped architecture is designed and synthesized by coordinating two square-planar-coordinated Pd^{2+} ions with four *trans*-azobenzene-containing bis-pyridyl ligands (azo-ligand). The azo-cage can be reversibly disassembled/reassembled mediated by the azo-ligand under visible and UV light irradiation.

In recent decades, research on creating variously defined self-assembled metallosupramolecular structures using metal–ligand coordination has experienced a boom.[1] Among these structures, metal–ligand M_2L_4 coordination cages, formed by pyridine-Pd^{2+} contacts that take advantage of the square-planar geometric metal ions Pd^{2+}, are interesting structures that have received considerable attention.[2] Owing to the unique properties of their cavities, these supramolecular systems have been widely exploited for molecular recognition and encapsulation,[3] catalysis,[4] and luminescent materials,[5] among others. Now, these stimuli-responsive metal–ligand coordination cages, in which the architectures can be switched, by external stimuli, are receiving much attention.[6] Controlling self-assembled architectures using external stimuli is of great importance. This can not only switch the structure of the cages, but also change their host–guest properties, which is particular important for the uptake, delivery, and release of cargo.[7] For example, Crowley and coworkers have recently reported the synthesis of stimuli-responsive Pd_2L_4 metallosupramolecular cages for targeted cisplatin drug delivery.[8] Severin also reported the reversible disassembly of metallosupramolecular structures mediated by a metastable-state photoacid.[9] Clever and coworkers also reported a family of light-triggered photochromic coordination cages that can undergo structure interconversions for light-triggered guest uptake and release.[10] However, the construction of stimuli-responsive M_2L_4 coordination cages has remained difficult. Expanding self-assembly to the construction of stimuli-responsive coordination cages is challenging, because: (i) designing supramolecular structures with responses to special stimuli, such as pH, temperature, and light, is challenging; (ii) the design and synthesis of organic ligands with stimuli responsive groups as directing units is challenging; and (iii) metal–ligand connectivity with a fixed geometry must be obtained.

Light is a particularly useful and efficient stimulus for causing reversible structural changes in supramolecular systems. Switching of supramolecular structures by light plays an important role in creating functional nanoscale devices.[11] Azobenzene, a photochromic molecule, has attracted particular interest owing to its high stability and UV-vis absorbance change under light stimulation.[12] Furthermore, the *cis*/*trans*-isomerization of azobenzene under light stimulation is especially attractive. Owing to their unique chemical and physical properties, azobenzenes have been widely used to construct smart optical switching materials.[13] Inspired by these outstanding studies, we aimed to design a new kind of metal–ligand coordination cage with azobenzene groups in the well-defined architecture regions, such that the metallosupramolecular assembly or disassembly of these structures could be reversibly manipulated through photoswitching.

Herein, we designed and synthesized a novel bis-pyridyl ligand (azo-ligand) with two azobenzene groups attached to its two arms (Scheme 1a). Under visible light, the azo-ligand showed a fixed conformation in the square-planar geometry to form M_2L_4 coordination cages.[14] Through the self-assembly of 1 equiv. of Pd^{2+} ions and 2 equiv. of azo-ligand, a novel azobenzene-containing light-stimuli-responsive metal–organic M_2L_4 cage (azo-cage) was prepared for the first time (Scheme 1b). As the *trans*/*cis* isomerization of the azo-ligand produced a significant conformational change, the *cis* azo-ligand conformation was not pre-organised to form discrete supramolecular architectures with Pd^{2+}, meaning that the azo-cage can disassemble under UV light. Furthermore, as the azo-ligand conformation showed good reversibility and repetitiveness for light switching, the self-assembly

State Key Laboratory of Supramolecular Structure and Materials, College of Chemistry, Jilin University, Changchun 130012, People's Republic of China. E-mail: junqiuliu@jlu.edu.cn

† Electronic supplementary information (ESI) available. See DOI: 10.1039/c9qm00160c

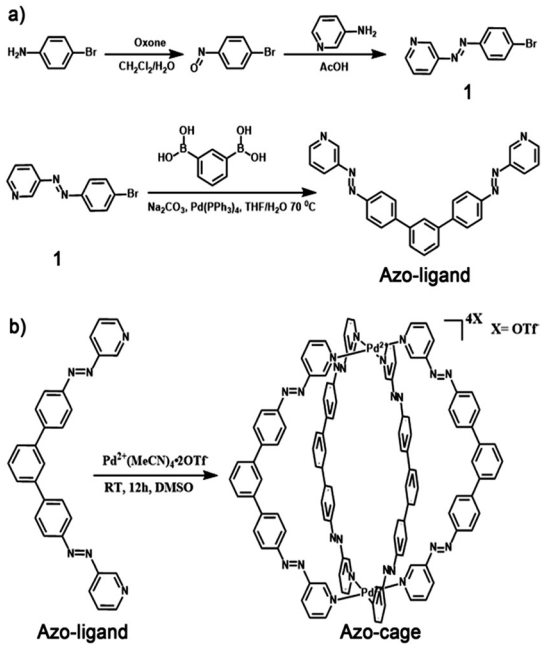

Scheme 1 (a) Design and synthesis of azo-ligand; (b) design and synthesis of light-stimuli-responsive metal–organic Pd_2L_4 cage (azo-cage).

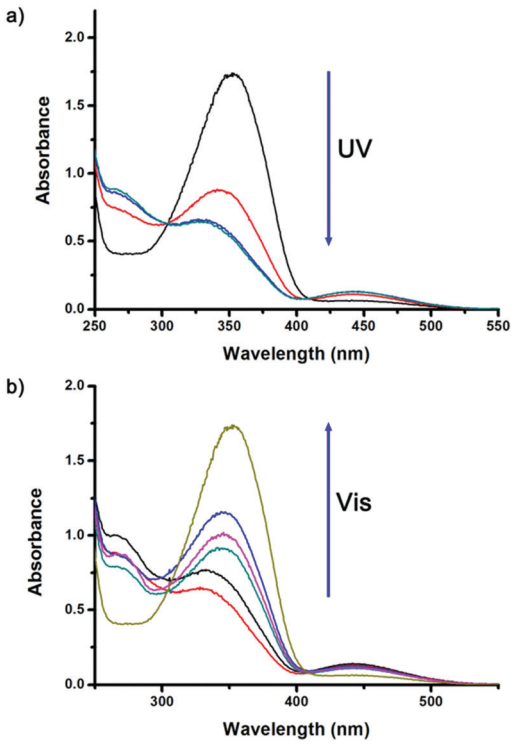

Fig. 1 UV-vis spectra (in $CHCl_3$) (a) under UV light irradiation and (b) under visible light irradiation again.

and disassembly coordination azo-cages were alternatively switched by visible and UV light.

Results and discussion

The light-stimuli-responsive azo-ligand was designed and synthesized using two steps, as shown in Scheme 1a. Initially, unsymmetrically substituted azobenzene **1** was synthesized and fully characterized (see ESI†). The azo-ligand was then prepared by the Suzuki–Miyaura cross-coupling ($Pd(PPh_3)_4$, K_2CO_3, THF/H_2O) of 1,3-benzenediboronic acid and azobenzene **1**. Details of the synthesis and characterization are shown in the ESI.†

Having successfully prepared the ligand, the reversibility of the light-controlled isomerization of the azo-ligand was investigated. The *trans*-ligand showed an absorption peak at 350 nm in $CDCl_3$ solution under visible light irradiation (Fig. 1a). Under UV light (365 nm) irradiation for 8 min, the azo-ligand showed an absorption intensity at 350 nm decreased from 1.73 to 0.53, and a new absorption peak appeared at 450 nm simultaneously (Fig. 1a), indicating the *trans*-ligand converting to the *cis*-isomer state with a transfer efficiency of 69%. The azo-ligand *cis*-isomer transformed back to the original *trans*-isomer under visible light irradiation (450 nm) (Fig. 1b). This photocontrolled isomerization of the azo-ligand was also monitored by NMR spectroscopy (Fig. S7, ESI†). Changes to the ^{1}H-NMR spectrum of the ligand in $CDCl_3$ upon irradiation with a 365 nm laser indicated that a mixture of isomers was formed, with proton peaks showing large changes, while some protons became complex multiplets (Fig. S8b and c, ESI†), and a new doublet appeared due to an increase in the shielding of aromatic protons in the azo groups of the *cis*-isomer. When the azo-ligand was irradiated with visible Light (450 nm), the ligand returned to its original *trans*-conformation, as confirmed by the ^{1}H-NMR spectrum. Furthermore, when the ligand was alternatively irradiated with UV/vis light, monitoring the absorption intensity at 350 nm, the azo-ligand showed good reversibility over several light-controlled isomerization cycles (Fig. S8, ESI†). All results indicated that the azo-ligand afforded good conformation reversibility for light-triggered isomerization.

Under visible light, with two *trans*-azobenzene groups attached at the two arms of the azo-ligand, we predicted a fixed geometry of the metal–ligand connectivity with Pd^{2+} to form well-defined M_2L_4 cage architectures (Scheme 1b). Here, simply adding $[Pd(CH_3CN)_4](OTf)_2$ (1 eq.) to a solution of the azo-ligand (2 eq.) in DMSO-d6 solution and stirring at room temperature for 2 h obtained the self-assembled coordination azo-cage complex (see Scheme 1b and ESI†). The azo-cage was first investigated using ^{1}H NMR spectroscopy in DMSO-d6. The ^{1}H NMR spectrum showed that all proton resonances were shifted downfield compared with those of the free azo-ligand (Fig. 2), owing to the lower electron density upon coordination with the Pd^{2+} metal ion. In particular, the most significant downfield shifts were observed for protons distributed adjacent to the coordinating nitrogen atoms (H_7, $\Delta\delta$ = 0.95 ppm and H_6, $\Delta\delta$ = 0.85 ppm). The other protons resonances were slightly shifted downfield. All integrals for protons on the ligand remained unchanged, and their peaks remained sharp and in one position, with no miscellaneous peaks appearing. These results indicated that the azo-ligand had successfully coordinated with Pd^{2+}, and that only one complex with a high degree of structural symmetry was obtained.

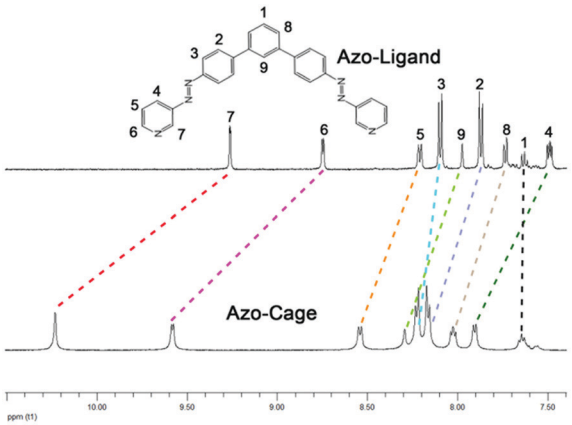

Fig. 2 (a) ^{1}H NMR spectra (DMSO-d, 298 K) of the azo-ligand and azo-cage; (b) ESI-TOF-MS spectra of azo-cage.

This self-assembled azo-cage was further characterized by ESI-MS (Fig. 3). The ESI-MS spectra (in CH_3CN solution) showed a series of isotopically resolved peaks consistent with the formula $[Pd_2(L)_4(OTf)_n]^{(4-n)+}$ (n = 0, 1, 2, 3) and peaks attributed to fragmentation of the cage structure. For the cage, MS signals were observed at m/z 493.6, 708.2, 1136.2, and 2422.1, attributed to $[Pd_2(L)_4]^{4+}$, $[Pd_2(L)_4(OTf)_1]^{3+}$, $[Pd_2(L)_4(OTf)_2]^{2+}$, and $[Pd_2(L)_4(OTf)_3]^{+}$ ions, respectively. Furthermore, the isotopic patterns of each resolved peak agreed well with the simulated values, which further confirmed the composition of the azo-cage. Many prominent fragmentation peaks were observed in the spectra owing to reduced stability of the cage architecture under the ES-MS experiment conditions.

Diffusion-ordered NMR spectroscopy (DOSY) was also employed to monitor formation of the self-assembly cage. The ^{1}H DOSY spectrum of the cage was obtained in DMSO solution at 298 K (Fig. 4a), and the proton signals in the spectrum showed a diffusion coefficient (D) of 8.53 $\times$ 10^{-11} m^2 s^{-1}. According to the Stokes–Einstein equation, the hydrodynamic radius can be calculated from the diffusion values as 12.9 Å. Further structural evidence was provided by 2D-COSY, HSQC, and HMBC experiments (see ESI†).

With the azo-cage characterized by NMR, DOSY, and MS techniques, it was desirable to obtain structural information for the cage. The theoretical model of the cage structure was constructed using Gauss View 5.0 (optimized by Gaussian 09) and Pymol software was used to display the molecular geometry of the azo-cage. As shown in Fig. S16 and S17 (ESI†), two structure models, A and B, were obtained. The two azo-cage models both featured lantern-shaped architectures. Model A had a cavity with a depth of 12.0 Å and width of 16.5 Å. The longest outer diameter was 25.8 Å (Fig. 4b), which agreed with the ^{1}H DOSY result for hydrodynamic diameter ($2r$ = 2 $\times$ 12.9 Å = 25.8 Å). Model B had a cavity with a depth of 14.3 Å and width of 12.6 Å, and a longest outer diameter of 24.5 Å. Furthermore, from thermodynamics calculations, model A was more stable than model B. This

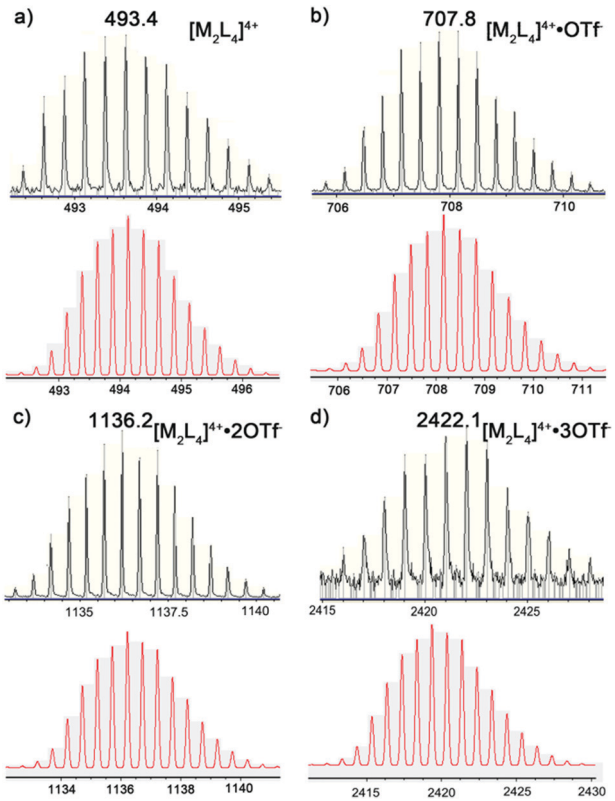

Fig. 3 ESI-TOF-MS spectra of azo-cage. Experimental (black) and theoretical (red) isotopic distributions: found (a) $([Pd_2(L)_4]^{4+}$ (493.9), (b) $[Pd_2(L)_4(OTf)_1]^{3+}$ (708.2), (c) $[Pd_2(L)_4(OTf)_2]^{2+}$ (1136.2), and d) $[Pd_2(L)_4(OTf)_3]^{+}$ (2422.1).

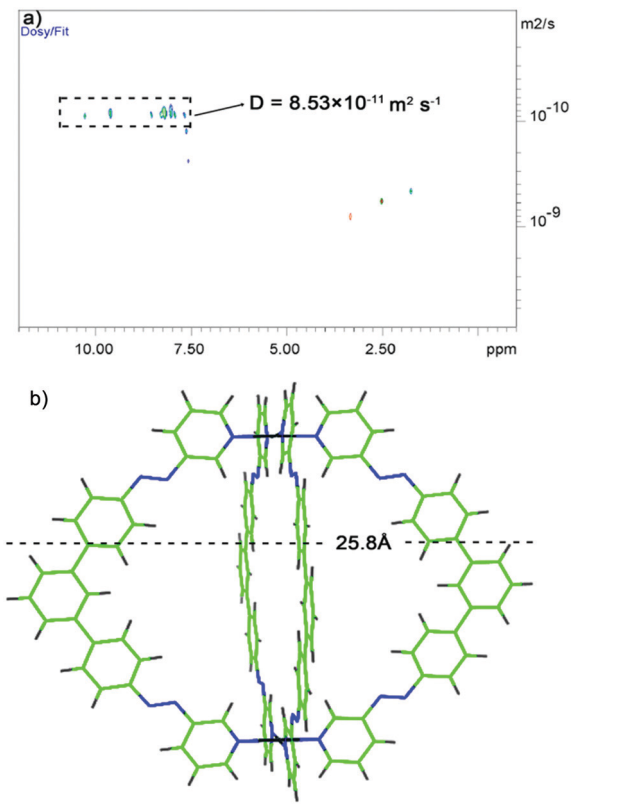

Fig. 4 (a) ^{1}H DOSY spectrum of the azo-cage; (b) theoretical model A of the azo-cage structure (blue bond is –N=N– group).

suggested that model A was more appropriate for the azo-cage structure.

The azo-cage was stable under visible light, but began to degrade when irradiated with UV light (365 nm). We used the UV-vis spectrum analysis method to monitor the degradation process. The UV-vis spectrum (Fig. 5a) clearly showed that, under UV light irradiation, the absorption intensity at 350 nm decreased from 1.62 to 0.43, indicating that the *trans*-ligand had partially converted to the *cis*-isomer, which induced structural changes in the self-assembled cage. If the system continued to be irradiated with UV light, an orange precipitate was generated (Fig. 5b). We separated and extracted the precipitate, and found that it was the free ligand (as confirmed by NMR and ESI-TOF analyses). ^{1}H NMR and ESI-MS analyses also gave clear evidence for degradation under UV light irradiation. Fig. 5c clearly shows that, after irradiation with UV light (until the precipitate formed), proton resonances in the ^{1}H NMR spectrum were disordered. In particular, the pyridinyl protons (see Fig. 5c-1 and c-2) were clearly shifted upfield. Other proton signals also changed (see Fig. 5c-3). Cage degradation under UV light was also confirmed by ESI-MS analysis *in situ*. The signals in the ESI-MS spectrum corresponding to the self-assembled cage disappeared after UV irradiation compared with those in the normal state, with only some fragments and azo-ligand generated (signals at 537.2 and 597.2) (Fig. S18, ESI†). Interestingly, when the disassembly system was irradiated with visible light again, the azo-ligand converted back to the *trans*-isomer and could reassemble with

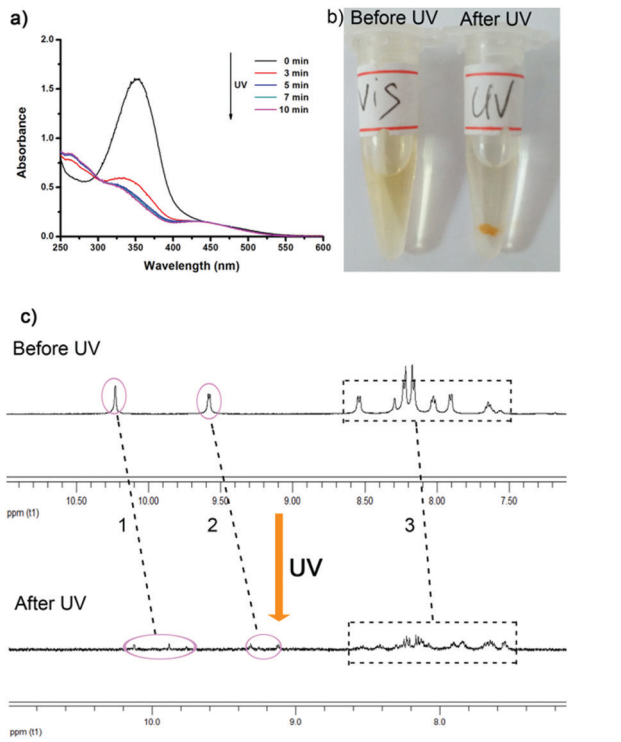

Fig. 5 (a) UV-vis spectra of azo-cage under UV light irradiation (in DMSO); (b) photograph of self-assembled sample under visible or UV light irradiation; (c) ^{1}H NMR spectra (DMSO-d, 298 K) of azo-cage under visible or UV light irradiation (from the same sample).

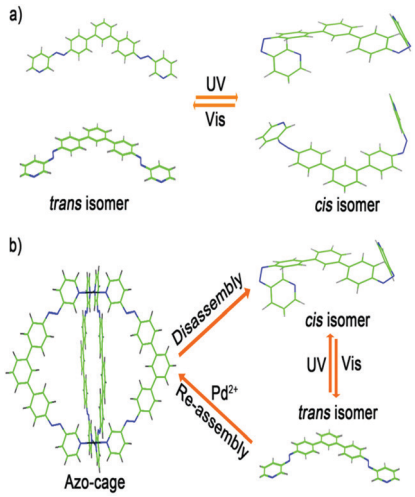

Fig. 6 (a) Theoretical simulation of the azo-ligand in *trans* or *cis* isomer states (blue bond is –N=N– group); (b) self-assembly and disassembly of azo-cage with light stimuli manipulation.

Pd^{2+} to form the Pd_2L_4 coordination cages (azo-cages) again, as confirmed by the UV-vis spectrum and ESI-TOF and NMR analyses (Fig. S19–S21, ESI†).

The photoswitching mechanism of assembly and disassembly of the azo-cage was further investigated. We first simulated the azo-ligand conformations to obtain *trans*- or *cis*-isomers. The results showed that *trans*/*cis* isomerization of the azo-ligand resulted in a huge conformational change (Fig. 6a). In the *trans*-isomer state, the azo-ligand had a suitable conformation to fix the geometry of metal–ligand connectivity for azo-cage. However, in the *cis*-isomer state, the conformations are disordered and not suitable for self-assembly with Pd^{2+} to form an azo-cage. To confirm the computer simulation, we designed a control experiment that proceeds through an opposite self-assembly. Firstly, the azo-ligand was irradiated with UV light until isomerization was thoroughly induced. $[Pd(CH_3CN)_4](OTf)_2$ was then added and the reaction was conducted under UV light in CD_3CN. The ^{1}H NMR spectrum (Fig. S22b and c, ESI†) showed that Pd^{2+} was coordinated with the ligand, because the protons near the coordinating nitrogen atoms had significantly shifted downfield. ESI-MS analysis was also used to judge the process *in situ*. As shown in Fig. S23 (ESI†), even when the reaction was prolonged for 5 h, no signal appeared that represented the formation of Pd_2L_4 coordination cages, while the free ligand and some prominent fragmentation peaks were observed in the spectra. When the system was subsequently irradiated with visible light, the *cis*-ligands switched back to *trans*-isomers. The ^{1}H NMR spectrum (Fig. S22a, ESI†) showed that Pd^{2+} was still coordinated with the ligand, while the ESI-MS spectrum confirmed regeneration of the azo-cage (Fig. S24, ESI†). The computer simulation and control experiment results clearly demonstrated that the major conformation change through *cis*/*trans*-isomerization of the azo-ligand played a key role in manipulating the photoisomerization of the assembly and disassembly processes of the azo-cage, as shown in Fig. 6b. Under visible light, the azo-ligand had a suitable conformation for the formation of fixed M_2L_4 cages

with square-planar coordination geometry, and assembled with Pd^{2+} to form well-defined azo-cages. However, under UV light, the azo-ligand can directly switch to the *cis*-isomer state, which has a disordered conformation, such that the azo-cage is not stable and disassembles. Furthermore, if the *cis*-isomer of the azo-ligand is converted back to the *trans*-isomer, the azo-cage can reform, which presents good reversibility and repetitiveness for the photoswitching self-assembly and disassembly of azo-cages.

Conclusions

In summary, we have developed a new light-stimuli-responsive coordination M_2L_4 cage through the quantitative self-assembly of photoisomerizable azobenzene-containing ligands and Pd^{2+} ions. ^{1}H-NMR, ESI-MS, DOSY, 2D-COSY, HSQC, HMBC, and theoretical simulation results supported the size, shape, composition, and cage structures. The self-assembly and disassembly coordination cages can be alternatively manipulated by photoswitching, which is attributed to the major conformation change caused by *cis*/*trans*-isomerization of azo-ligand. This work not only reports a new type of stimuli-responsive coordination cage, which might be useful in targeted release, but also provides a new approach for the design of intelligent nanomaterials.

Conflicts of interest

There are no conflicts of interest to declare.

Acknowledgements

This work was supported by the National Natural Science Foundation of China (No. 21420102007, 21574056, and 91527302) and the JLU Science and Technology Innovative Research Team.

Notes and references

1 Q.-F. Sun, J. Iwasa, D. Ogawa, Y. Ishido, S. Sato, T. Ozeki, Y. Sei, K. Yamaguchi and M. Fujita, *Science*, 2010, **328**, 1144; D. Fujita, Y. Ueda, S. Sato, N. Mizuno, T. Kumasaka and M. Fujita, *Nature*, 2016, **540**, 563; D. Fujita, Y. Ueda, S. Sato, H. Yokoyama, N. Mizuno, T. Kumasaka and M. Fujita, *Chem*, 2016, **1**, 91; T. R. Cook and P. J. Stang, *Chem. Rev.*, 2015, **115**, 7001; B. Sun, M. Wang, Z. Lou, M. Huang, C. Xu, X. Li, L. Chen, Y. Yu, G. L. Davis, B. Xu, H. B. Yang and X. Li, *J. Am. Chem. Soc.*, 2015, **137**, 1556; Z. Jiang, Y. Li, M. Wang, B. Song, K. Wang, M. Sun, D. Liu, X. Li, J. Yuan, M. Chen, Y. Guo, X. Yang, T. Zhang, C. N. Moorefield, G. R. Newkome, B. Q. Xu and X. Li, *Nat. Commun.*, 2017, **8**, 15476; H. Wang, X. Qian, K. Wang, M. Su, W. Haoyang, X. Jiang, R. Brzozowski, M. Wang, X. Gao, Y. Li, B. Q. Xu, P. Eswara, X. Hao, W. Gong, J.-L. Hou, J. Cai and X. Li, *Nat. Commun.*, 2018, **9**, 1815.

2 M. Fujita, M. Tominaga, A. Hori and B. Therrien, *Acc. Chem. Res.*, 2005, **38**, 371; A. Schmidta, A. Casinib and F. E. Kühna, *Coord. Chem. Rev.*, 2014, **275**, 19; M. Wang, C. Wang, X.-Q. Hao, X. Li, T. J. Vaughn, Y.-Y. Zhang, Y. Yu, Z.-Y. Li, M.-P. Song, H.-B. Yang and X. Li, *J. Am. Chem. Soc.*, 2014, **136**, 10499; Q.-F. Sun, S. Sato and M. Fujita, *Nat. Chem.*, 2012, **4**, 330; B. S. Pilgrim and J. R. Nitschke, *Chem*, 2016, **1**, 16; P. Liao, B. W. Langloss, A. M. Johnson, E. R. Knudsen, F. S. Tham, R. R. Julian and R. J. Hooley, *Chem. Commun.*, 2010, **46**, 4932; Y. Liu, B. Shi, H. Wang, L. Shangguan, Z. Li, M. Zhang and F. Huang, *Macromol. Rapid Commun.*, 2018, **39**, 1800655.

3 D. P. August, G. S. Nichol and P. J. Lusby, *Angew. Chem., Int. Ed.*, 2016, **55**, 1; K. Yazaki, M. Akita, S. Prusty, D. K. Chand, T. Kikuchi, H. Sato and M. Yoshizawa, *Nat. Commun.*, 2017, **8**, 15914; B. M. Schmidt, T. Osuga, T. Sawada, M. Hoshino and M. Fujita, *Angew. Chem., Int. Ed.*, 2016, **55**, 1561; D. Fujita, K. Suzuki, S. Sato, M. Yagi-Utsumi, Y. Yamaguchi, N. Mizuno, T. Kumasaka, M. Takata, M. Noda, S. Uchiyama, K. Kato and M. Fujita, *Nat. Commun.*, 2012, **3**, 1093; N. Kishi, Z. Li, K. Yoza, M. Akita and M. Yoshizawa, *J. Am. Chem. Soc.*, 2011, **133**, 11438.

4 M. Yoshizawa, M. Tamura and M. Fujita, *Science*, 2006, **312**, 251; K. Yan and M. Fujita, *Science*, 2015, **350**, 1165; Y. Ueda, H. Ito, D. Fujita and M. Fujita, *J. Am. Chem. Soc.*, 2017, **139**, 6090; V. Martí-Centelles, A. L. Lawrence and P. J. Lusby, *J. Am. Chem. Soc.*, 2018, **140**, 2862; L. R. Holloway, P. M. Bogie, Y. Lyon, C. Ngai, T. F. Miller, R. R. Julian and R. J. Hooley, *J. Am. Chem. Soc.*, 2018, **140**, 8078.

5 S. S. Babu, M. J. Hollamby, J. Aimi, H. Ozawa, A. Saeki, S. Seki, K. Kobayashi, K. Hagiwara, M. Yoshizawa, H. Möhwald and T. Nakanishi, *Nat. Commun.*, 2013, **4**, 1969; M. Yamashina, M. M. Sartin, Y. Sei, M. Akita, S. Takeuchi, T. Tahara and M. Yoshizawa, *J. Am. Chem. Soc.*, 2015, **137**, 9266; X. Yan, T. R. Cook, P. Wang, F. Huang and P. J. Stang, *Nat. Chem.*, 2015, **7**, 342; M. Zhang, M. L. Saha, M. Wang, Z. Zhou, B. Song, C. Lu, X. Yan, X. Li, F. Huang, S. Yin and P. J. Stang, *J. Am. Chem. Soc.*, 2017, **139**, 5067; C. Lu, M. Zhang, D. Tang, X. Yan, Z. Zhang, Z. Zhou, B. Song, H. Wang, X. Li, S. Yin, H. Sepehrpour and P. J. Stang, *J. Am. Chem. Soc.*, 2018, **140**, 7674.

6 A. J. McConnell, C. S. Wood, P. P. Neelakandan and J. R. Nitschke, *Chem. Rev.*, 2015, **115**, 7729; S.-S. Sun, J. A. Anspach and A. J. Lees, *Squares. Inorg. Chem.*, 2002, **41**, 1862; I. X. Green, W. Tang, M. Neurock and J. T. Yates Jr, *J. Am. Chem. Soc.*, 2012, **134**, 13569; T. Y. Kim, R. A. S. Vasdev, D. Preston and J. D. Crowley, *Chem. – Eur. J.*, 2018, **24**, 14878.

7 P. Mal, D. Schultz, K. Beyeh, K. Rissanen and J. R. Nitschke, *Angew. Chem., Int. Ed.*, 2008, **47**, 8297; N. Kishi, M. Akita, M. Kamiya, S. Hayashi, H.-F. Hsu and M. Yoshizawa, *J. Am. Chem. Soc.*, 2013, **135**, 12976; I. A. Riddell, M. M. J. Smulders, J. K. Clegg and J. R. Nitschke, *Chem. Commun.*, 2011, **47**, 457; D. Preston, A. Fox-Charles, W. K. C. Lo and J. D. Crowley, *Chem. Commun.*, 2015, **51**, 9042.

8 J. E. M. Lewis, E. L. Gavey, S. A. Cameron and J. D. Crowley, *Chem. Sci.*, 2012, **3**, 778.

9 S. M. Jansze, G. Cecot and K. Severin, *Chem. Sci.*, 2018, **9**, 4253.

10 M. Han, R. Michel, B. He, Y.-S. Chen, D. Stalke, M. John and G. H. Clever, *Angew. Chem., Int. Ed.*, 2013, **52**, 1319; M. Han,

Y. Luo, B. Damaschke, L. Gómez, X. Ribas, A. Jose, P. Peretzki, M. Seibt and G. H. Clever, *Angew. Chem., Int. Ed.*, 2016, **55**, 445.

11 M. Irie, T. Fukaminato, K. Matsuda and S. Kobatake, *Chem. Rev.*, 2014, **114**, 12174; A. J. McConnell, C. S. Wood, P. P. Neelakandan and J. R. Nitschke, *Chem. Rev.*, 2015, **115**, 7729.

12 A. Natansohn and P. Rochon, *Chem. Rev.*, 2002, **102**, 4139; W. Szymański, J. M. Beierle, H. A. V. Kistemaker, W. A. Velema and B. L. Feringa, *Chem. Rev.*, 2013, **113**, 6114; A. S. Lubbe, W. Szymanski and B. L. Feringa, *Chem. Soc. Rev.*, 2017, **46**, 1052; Y. Kitamura, R. Ichikawa and H. Nakano, *Mater. Chem. Front.*, 2018, **2**, 90; K. Wang, L. Yin, T. Miu, M. Liu, Y. Zhao, Y. Chen, N. Zhou, W. Zhang and X. Zhu, *Mater. Chem. Front.*, 2018, **2**, 1112; X. Yu, H. Chen, X. Shi, P.-A. Albouy, J. Guo, J. Hu and M.-H. Li, *Mater. Chem. Front.*, 2018, **2**, 2245.

13 T. Murase, S. Sato and M. Fujita, *Angew. Chem., Int. Ed.*, 2007, **46**, 5133; P. V. D. Asdonka and P. H. J. Kouwer, *Chem. Soc. Rev.*, 2017, **46**, 5935; P. Mondal, G. Granucci, D. Rastädter, M. Persico and I. Burghardt, *Chem. Sci.*, 2018, **9**, 4671; L. Albert, J. Xu, R. Wan, V. Srinivasan, Y. Dou and O. Vazquez, *Chem. Sci.*, 2017, **8**, 4612; H. Sun, L. Zhao, T. Wang, G. An, S. Fu, X. Li, X. Deng and J. Q. Liu, *Chem. Commun.*, 2016, **52**, 6001; H. Wang, C. N. Zhu, H. Zeng, X. Ji, T. Xie, X. Yan, Z. L. Wu and F. Huang, *Adv. Mater.*, 2019, **31**, 1807328.

14 D. K. Chand, K. Biradha and M. Fujita, *Chem. Commun.*, 2001, 1652; G. H. Clever, S. Tashiro and M. Shionoya, *Angew. Chem., Int. Ed.*, 2009, **121**, 7144; G. H. Clever and P. Punt, *Acc. Chem. Res.*, 2017, **50**, 2233.